Percolation and cooperation with mobile agents: Geometric and strategy clusters

Mendeli H. Vainstein,[*] Carolina Brito,[†] and Jeferson J. Arenzon[‡]
Instituto de Física, Universidade Federal do Rio Grande do Sul, C.P. 15051, 91501-970 Porto Alegre RS, Brazil
(Received 30 June 2014; published 26 August 2014)

We study the conditions for persistent cooperation in an off-lattice model of mobile agents playing the Prisoner's Dilemma game with pure, unconditional strategies. Each agent has an exclusion radius r_P, which accounts for the population viscosity, and an interaction radius r_{int}, which defines the instantaneous contact network for the game dynamics. We show that, differently from the $r_P = 0$ case, the model with finite-sized agents presents a coexistence phase with both cooperators and defectors, besides the two absorbing phases, in which either cooperators or defectors dominate. We provide, in addition, a geometric interpretation of the transitions between phases. In analogy with lattice models, the geometric percolation of the contact network (i.e., irrespective of the strategy) enhances cooperation. More importantly, we show that the percolation of defectors is an essential condition for their survival. Differently from compact clusters of cooperators, isolated groups of defectors will eventually become extinct if not percolating, independently of their size.

DOI: 10.1103/PhysRevE.90.022132 PACS number(s): 02.50.Le, 87.23.Ge, 64.60.ah

I. INTRODUCTION

Network reciprocity [1,2] is a general mechanism responsible for the development of spatial correlations within a viscous population, opening the possibility of persistent cooperation. Several specific models have been proposed showing how these correlations are related to stable groups of cooperating individuals, whose bulk benefits of self-defense and mutual support outcompete the surface exploitation by defectors [3–7]. Although actual experiments have been performed [8–11], most of our knowledge comes from these simple models. In particular, a prevailing characteristic in real systems, and an important ingredient for cooperation, is the heterogeneous contact in systems whose interactions are given by complex [12,13] or diluted [14] networks. When we consider the Prisoner's Dilemma (PD) dynamics [1] on a diluted lattice that, albeit heterogeneous, has only short-range interactions, intermediate densities present an enhancement of cooperation [14–16], and in the presence of a small amount of noise, the optimal dilution is closely related to the (random-site) percolation threshold for that lattice [16].

Whatever the level of heterogeneity, the contact network topology may evolve in time. Although several rewiring mechanisms can be devised (see Ref. [7] and references therein), this may also be accomplished when the high-viscosity restriction is relaxed and the agents become mobile. Mobility patterns on different scales of human activity, and their far-fetched consequences, have been studied in recent decades. For example, airplane displacement and its connection with disease spread [17], on a global level, can be contrasted with the more local dynamics of pedestrians, crowds, or traffic [18,19]. Of particular interest is how the observed patterns can affect the outcome of the competition between agents and, in turn, be influenced by it as well. Within the evolutionary game theory framework, after several sparse, early attempts to include mobility [20–27], it was only recently that the interest in the combined effects of mobility and cooperation in the PD game had a significant increase. Some level of information processing capability is required, for example, when the movement is strategy dependent [28,29] or driven by payoff [30–33], success [34–37], or neighborhood composition [38–45]. However, the simplest scenario is when mobility is diffusive [29,46–53]. Indeed, as hypothesized in Refs. [46,54], random mobility may have evolved prior to contingent mobility, allowing bacteria to move away from each other while exploring new resources. Our previous results on a lattice [46,48,55] show that, even in the framework of random, noncontingent mobility of unconditional agents, diffusion is favorable to cooperation, under rather broad conditions, if velocities are not too high. Analogous conclusions, attesting the robustness of the results, were also found in off-lattice models [45,49,56].

When diffusion occurs on a lattice and the one agent per site constraint holds, this area exclusion couples the diffusivity of the agents with the free area. This dependence on density, on the other hand, is not immediately present in off-lattice systems with point-like particles [33,42,45,49,56]. Moreover, whereas on a lattice the number of simultaneous interactions is limited by its coordination number, there is no such restriction on the number of point-like particles within the range of interactions in off-lattice systems (unless it is explicitly included as in Ref. [45]). A relevant question concerns the universal effects of such a geometrical hindrance on the emergence and persistence of cooperation. For example, letting the average body size be a coevolving trait, there may be some evolutive pressure for not too small cooperators because, assuming random diffusion, a group of small individuals will more easily evaporate from the cluster surface. They should not be too large either and, consequently, not be able to evade defectors and avoid exploitation. Analogously, for defectors, they should neither be too small, in order to stay closer to their prey for longer periods, nor too large, so that new, more promising regions will not be explored. Therefore, one intuitively expects that intermediate, optimal sizes may be beneficial to cooperation and thus be selected for. Another possible interpretation for an exclusion zone around each agent is its protected region, and the resources within. Whatever the interpretation, it is

[*]vainstein@if.ufrgs.br
[†]carolina.brito@ufrgs.br
[‡]arenzon@if.ufrgs.br

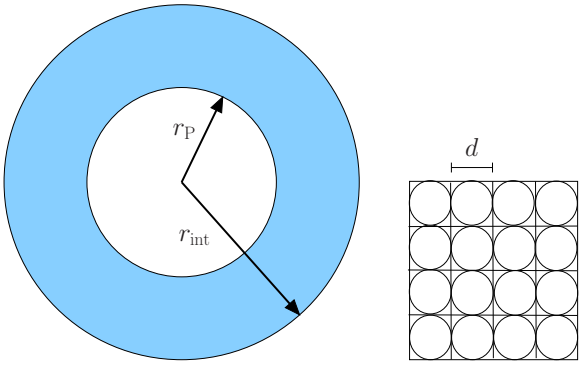

FIG. 1. (Color online) Geometric parameters of the model, the hard-core radius r_P, and the interaction radius r_{int}. While the former sets an exclusion area around each agent, the latter defines its contact network. The characteristic length d, as indicated at the right, is defined by dividing the available area, L^2, by the area of the square box around each of the N particles of diameter d, that is, $L^2/d^2 = N$.

important to better understand the relevance of area exclusion in these games. As a first approximation, we consider an effective radius of exclusion, modeled as a hard disk.

Here we study, by explicitly taking into account the excluded area of the agents, the interplay among geometry, density, and mobility on the capability of a simple model to sustain cooperation and the question of whether the transitions in this class of model have a geometric interpretation. Although the connection between the threshold of geometric percolation, which is independent of the game dynamics, and cooperation has been reported in Refs. [16], [57], and [58], we also explore the geometry of clusters of cooperators and defectors, and the connection between their critical properties and the transition between regions with and without cooperation, thus providing a geometric interpretation of these transitions.

II. THE MODEL

We study an off-lattice model [45,49,59] in which the N agents living in a square of side L (with periodic boundary conditions) are characterized by an unconditional strategy (cooperate, C, or defect, D) and two independent geometric parameters: an interaction radius r_{int} and a hard disk radius r_P to account for excluded area. The radius r_{int} determines the neighborhood of each agent and, as a consequence, its instantaneous contact network. The area fraction occupied by the hard disk particles is $\phi = N\pi r_P^2/L^2$. We use $d \equiv L/\sqrt{N}$ as our length scale. These geometric parameters are illustrated in Fig. 1. The particular case studied by Meloni *et al.* [49] is recovered in the limit of point-like particles, $r_P = 0$.

Initially, N individuals with probability $1/2$ of being either C or D are randomly placed in such a way that there is no overlap between any two individuals i and j; i.e., their center-to-center distance r_{ij} satisfies $r_{ij} \geqslant 2r_P$. Moreover, they are allowed to randomly diffuse while playing the PD game with their neighbors. Two agents are considered neighbors if $r_{ij} < r_{int}$. A time step is defined as a sequence of N attempts of diffusion and a complete, synchronous round of the PD in which each of the N agents plays with all its neighbors. During the diffusive part, the position (x_i, y_i) of the center of particle i at time t is updated if there is no overlap between particles in the final position:

$$x_i(t+1) = x_i(t) + \mu r_{int}\cos\theta_i(t),$$
$$y_i(t+1) = y_i(t) + \mu r_{int}\sin\theta_i(t).$$

Each step has a constant size μr_{int} and a random orientation $\theta_i(t)$ drawn from a uniform distribution in the interval $[-\pi,\pi]$. When $\mu = 0$ there is no mobility and we consider here that μ is small enough so that jumps over other agents do not occur. Under mutual cooperation (defection), both receive payoff R (P) as a reward (punishment); if one cooperates and the other defects, then the latter receives T (temptation) and the former, S. To characterize the PD, the following inequalities should hold $T > R > P \geqslant S$ and $2R > T + S$. In particular, we use $R = 1$, $P = S = 0$, and $T > 1$, a common parametrization known as the weak form of the PD game. The evolution follows the finite-population analog of the replicator dynamics [13]. Each individual i, after accumulating the payoff from all combats, randomly chooses a neighbor j with whom to compare his or her respective payoffs P_i and P_j. If $P_i \geqslant P_j$, then i maintains its strategy. On the other hand, if $P_j > P_i$, i will adopt the strategy of j with a probability proportional to the payoff difference,

$$\Pi_{ij} = \frac{P_j - P_i}{\max\{k_j,k_i\}T}, \tag{1}$$

where k_i and k_j are the number of neighbors of i and j, respectively. Under this update rule, the total number of individuals is kept constant.

Most of our results are for $N = 32^2$, $T = 1.1$, $\mu = 0.01$, and $L = 1$. We then check the robustness of the model by testing finite-size effects with up to $N = 128^2$ particles, as well as the dependence on T and μ. Averages are taken over 100 or more samples.

III. COOPERATION AND PERCOLATION

Two macroscopic asymptotic quantities, once averaged, are used to characterize the system: the fraction of cooperators ρ_C (those, among the N agents, that cooperate) and the fraction $f_C \leqslant \rho_C$ of initial conditions whose evolution ends in the absorbing state $\rho_C = 1$. Their difference, $\rho_C - f_C$, is a measure of the coexistence of both strategies. Four regimes are present in the time evolution, as shown by the behavior of $\rho_C(t)$ in Fig. 2. As is often the case for this class of model, there is an initial drop in the fraction of cooperators from $\rho_C(0) = 1/2$, since small cooperator clusters are easily preyed on in the beginning of the simulation. As $\rho_C(t)$ approaches its minimum value at $t \sim 10^2$, fluctuations may lead to extinctions in finite-size systems. Away from the minimum, the surviving clusters of cooperators resume growth. These two initial regimes are quite independent of the occupied area fraction, as indicated in Fig. 2 by the close proximity of all curves up to $t \sim 10^3$. In the third regime, $\rho_C(t)$ attains a plateau where it stays, indicating the persistent coexistence of both strategies, if ϕ is large enough (in the case of Fig. 2, the threshold is at $\phi \simeq 0.37$). When ϕ is below the threshold, after the stasis period on the plateau, the system enters the last regime, in which cooperators take over the system, that is, $\rho_C(\infty) = 1$.

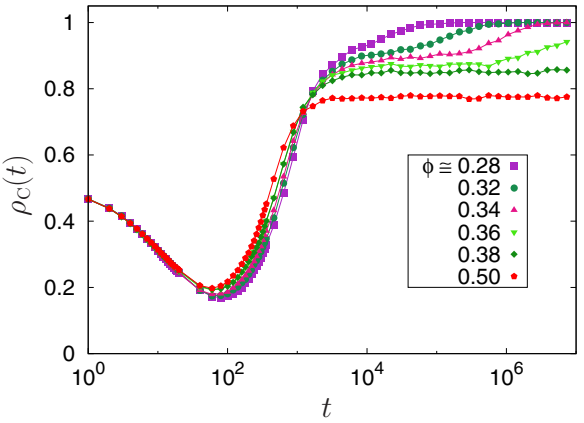

FIG. 2. (Color online) Average fraction of cooperators as a function of time (in Monte Carlo steps). $N = 32^2$, $T = 1.1$, $r_{\rm int} = \sqrt{3.5}d$, and $\mu = 0.01$ for various area fractions ϕ. Below $\phi \simeq 0.37$, cooperators eventually invade the whole system. As ϕ approaches this threshold, the time spent close to the critical plateau at $\rho_C \simeq 0.85$ also increases.

The time to reach this asymptotic state seems to diverge as the threshold area fraction is approached from below.

Figure 3 summarizes our most important results, showing, in the stationary regime, the average fraction of cooperators ρ_C as a function of both $r_{\rm int}/d$ and ϕ. The lines are independent measures of percolative properties that are explained below. Several regimes may be identified: two absorbing phases, in which all agents eventually become either defectors ($\rho_C = f_C = 0$; labeled D) or cooperators ($\rho_C = f_C = 1$; labeled C); and two coexistence ones ($0 < \rho_C < 1$ and $f_C = 0$; labeled C and D). Finite systems may also present a bistable phase, in which all initial conditions lead to one of the absorbing states. In this case, although the average cooperativeness still obeys $0 < \rho_C < 1$, it differs from the coexistence state since $f_C = \rho_C$. However, with an increase in the system size, the probability of becoming dominated by defectors goes to 0 inside the C region in Fig. 3, and taking this into account (see Fig. 5), we have already properly labeled it. We now

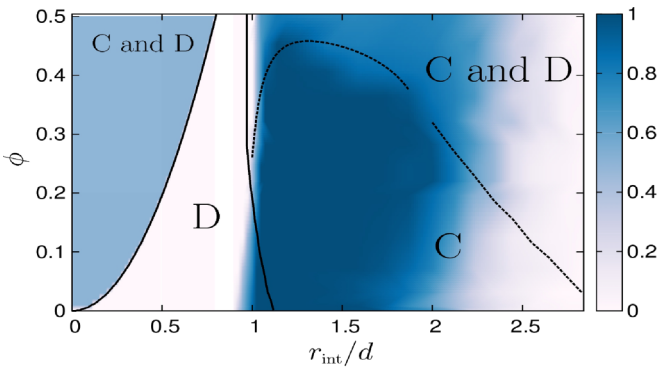

FIG. 3. (Color online) Phase diagram in the plane $r_{\rm int}/d$ and ϕ for $N = 32^2$, $\mu = 0.01$, and $T = 1.1$. The color code is the average fraction of cooperators, ρ_C. Besides the phases corresponding to the absorbing states, C ($\rho_C = f_C = 1$) and D ($\rho_C = f_C = 0$), there are two coexistence phases, C and D.

concentrate on the results for a finite system with $N = 32^2$ particles and then discuss the finite-size effects at the end of this section.

There are two limits of the diagram that have trivial results. For very large values of $r_{\rm int}$, very distant particles interact, increasing the number of contacts and decreasing the effects of spatial correlation. Thus, we recover the mean-field result in which all agents become defectors. This trivial region of the phase diagram was not explored. In the other limit, when $r_{\rm int} < 2r_P$, the hard core prevents any interaction between the agents and the fraction of cooperators remains equal to the initial one, $\rho_C = 1/2$ and $f_C = 0$. This is the trivial coexistence region, labeled C and D at the left in Fig. 3, above the line $\phi = (\pi/4)(r_{\rm int}/d)^2$, corresponding to $2r_P = r_{\rm int}$. Immediately to the right of this line, interaction, albeit weak, is possible and clusters are formed. However, they are small and do not favor cooperation, therefore $\rho_C = 0$, and this all-defector phase is labeled D. As we discuss below, the transitions between the other phases have geometric origins and are closely related to the percolating properties of the contact networks.

A. Geometric percolation

For the area fractions considered here, nontrivial cooperation first appears around $r_{\rm int} \approx d$. For small ϕ, the transition from phase D to phase C corresponds to a change in stability of the absorbing state, from the defector- to the cooperator-dominated phase, while for larger ϕ, roughly $\phi > 0.25$, the emergent phase is one in which cooperators and defectors coexist, C and D. This onset of cooperation is strongly correlated with the appearance of a *geometric* percolating cluster, indicated by the steep line in Fig. 3 at the point where the probability of finding a percolating cluster is 50%. This is a purely geometric problem of disks with both an inner hard core and a soft, penetrable region and, thus, independent of the game dynamics. In other words, the network of contacts of the percolating cluster spans the whole length of the system. For $\phi = 0$, our result is consistent both with the percolation threshold obtained numerically in Refs. [60] and [61] and with the exact bounds in Ref. [62]. For finite ϕ, the threshold is slightly smaller than for $\phi = 0$, since as r_P increases, the overlap between the disks decreases and percolation is attained with a smaller $r_{\rm int}$.

B. Percolating clusters of defectors

Besides the clusters of particles, irrespective of their strategies, we also consider the geometry of clusters composed only of defectors (which are, in turn, intimately connected with the geometry of cooperator clusters), which depends on the particular strategy evolving dynamics. Figure 4 shows the probability of percolation of D clusters as a function of time, $P_D(t)$, for $r_{\rm int} = \sqrt{3.5}d$. Note that in this region there is always a percolating geometric cluster. Initially, as the fraction of cooperators decreases towards the minimum, there is a sea of defectors that obviously percolates and all curves overlap at $P_D = 1$. It is only when the curves of $\rho_C(t)$, for different values of ϕ, start to separate, around $t \sim 10^3$, that $P_D(t)$ starts decreasing. The asymptotic probability of there being a percolating cluster of defectors attains a limiting value, as

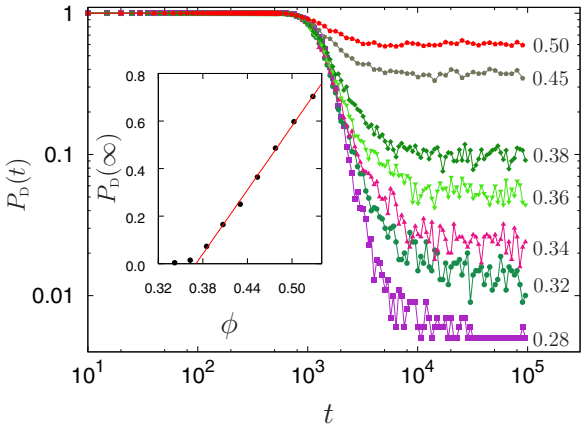

FIG. 4. (Color online) Probability of percolation of D clusters as a function of time, $P_D(t)$, for several area fractions ϕ and the same parameters as in Fig. 2. Inset: Asymptotic limit of $P_D(t)$ as a function of ϕ. The linear fit indicates that the percolation probability goes to 0 at $\phi \simeq 0.37$. The small deviation seen close to this point is due to the long time of convergence.

shown in the inset in Fig. 4, from which the threshold can be obtained. For the particular value of r_{int} shown in this figure, when the area fraction is below the threshold at (roughly) 0.37, $P_D(\infty) = 0$ and, as shown in Fig. 2, $\rho_C(\infty) = 1$. The dotted transition line in the phase diagram (Fig. 3) is obtained in the same manner: it is the asymptotic value of ϕ at which $P_D(\infty) = 0$ as a function of r_{int}. In the C region, finite-size fluctuations sometimes lead to the all-D state ($r_{\text{int}}/d \gtrapprox 2$), but these configurations are not taken into account for the calculation of the asymptotic value of ϕ. This transition line suggests an important ingredient for understanding the coexistence between cooperators and defectors: only under the presence of a percolating sea of defectors is a stable coexistence between cooperators and defectors possible. In other words, differently from compact clusters of cooperators, isolated groups of defectors either grow and percolate or eventually become extinct.

C. Finite-size effects

We now discuss how the system size can affect the phase diagram (Fig. 3). For finite-sized systems, a small region inside the C phase has a bistable equilibrium, in which all initial conditions lead to an absorbing state, either $\rho_C = 0$ or $\rho_C = 1$. The all-D state is due to the fact that the population of cooperators becomes quite small during the initial drop in the first generations and, therefore, sensitive to fluctuations which occasionally cause extinctions. Figure 5 shows f_C for two values of ϕ and several system sizes. For point particles ($\phi = 0$), the absorbing all-C-state region grows as the system size increases. On the other hand, for ($\phi \approx 0.28$), the all-C region shrinks. In both cases, however, the C-phase width converges to a finite value and the bistable region decreases as the system size increases. Furthermore, the size of the C region in the limit of large systems is consistent with the transition line obtained from the percolating defector cluster analysis for $N = 32^2$, which explains why this phase is not homogeneously colored in Fig. 3. Note that when the system is bistable, the

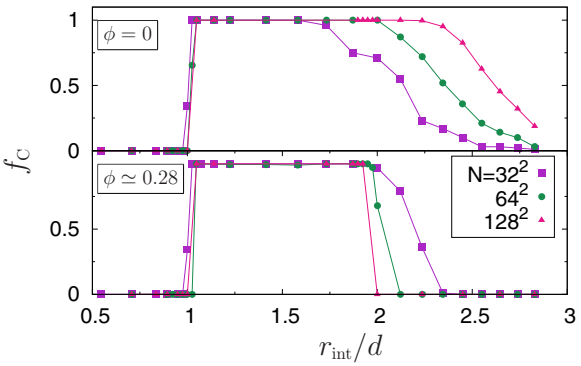

FIG. 5. (Color online) Fraction of initial states that go to the $\rho_C = 1$ absorbing state as a function of r_{int}/d for several system sizes and two area fractions, $\phi = 0$ and 0.28. For large values of r_{int}/d, as f_C increases for larger system sizes, the existence of the $\rho_C = 0$ state for point particles ($\phi = 0$) is due to finite-size fluctuations. For $\phi \simeq 0.28$ the behavior is the opposite and the transition becomes sharper when the system size increases.

average fraction of cooperators is not a good measure since it represents neither one of the final states [63]. On the other hand, in the coexistence state, both strategies are present in the asymptotic state, and while $0 < \rho_C < 1$, $f_C = 0$. For the $r_P = 0$ case studied by Meloni *et al.* [49], the $\phi = 0$ line in the phase diagram, there is no coexistence phase and the system eventually enters an absorbing state.

D. Robustness against mobility and temptation

We finally consider the robustness of our results when the mobility μ and the temptation T are varied (Fig. 6). The top panel in Fig. 6 shows several values of μ, with the temptation fixed at $T = 1.1$. Whatever the velocity, no cooperation is possible for $r_{\text{int}} \leqslant d$ due to the absence of a percolating geometric cluster. Nevertheless, for low mobilities, the existence of cooperators is possible in a wide range of r_{int}. Comparing the low mobility case with the case of immobile agents ($\mu = 0$), it can be seen that there is an improvement only for low values of the r_{int}/d ratio. For high values of this ratio, the curves overlap, which is expected, since the agents

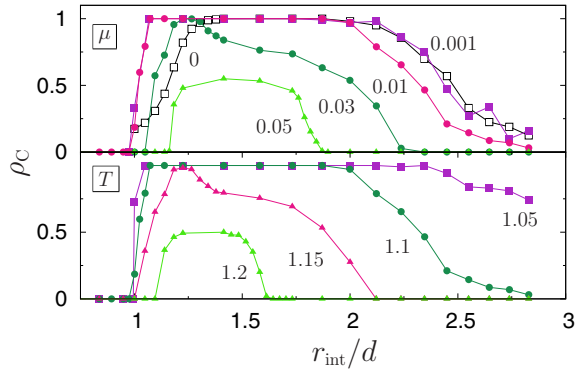

FIG. 6. (Color online) Average asymptotic fraction of cooperators as a function of r_{int}/d for $\phi \simeq 0.28$ and several values of μ (top), including $\mu = 0$ (open symbols), and T (bottom). In both cases, $N = 32^2$. Top, $T = 1.1$; bottom, $\mu = 0.01$.

have a large neighborhood that is minimally perturbed by the small random movements. On the other hand, for low values of the ratio, the contact range is small and is more affected by the diffusion. Random movements lead to the evaporation of cooperative clusters, and as the velocity increases, cooperation levels decrease until a threshold above which it is no longer possible. This effect of cooperation enhancement driven by a low mobility is in accordance with previous simulations on a lattice [46,48,49,55]. The bottom panel in Fig. 6 shows the effect of the parameter T. As expected, as the temptation to defect increases, the fraction of cooperators decreases.

IV. DISCUSSION AND CONCLUSION

We have presented numerical results for an off-lattice model of mobile agents playing the PD game while randomly moving across a closed region. This model combines ingredients found in two distinct models for such systems: the excluded area found in lattice simulations and an available continuous space. We arrive at two important results: first, if the agents are not point-like, a nontrivial coexistence phase with cooperators and defectors becomes possible (besides the trivial one when the exclusion range is larger than the interacting radius); second, it is possible to geometrically interpret, in terms of percolation, the observed transitions. An important role is played not only by geometric percolation, irrespective of the game dynamics, but also by the percolative properties of defector clusters, whose threshold depends on the details of the game.

When the agents' interaction is prevented by the hard core, trivial coexistence between cooperators and defectors is possible. Beyond that region of the phase diagram, no cooperation is possible in the absence of a percolating geometric cluster. Random mobility provides an evaporating mechanism for groups of cooperators that is detrimental to cooperation, as isolated cooperators are easily preyed on. However, in the presence of a percolating cluster, it is easier for a detaching cooperator to be in contact with another cluster and be protected. When hard cores are included, movements are hindered and the agents spend some time rattling around the same region, while large displacements become less probable, which increases the correlation among agents and benefits cooperation even further. This localization is probably the mechanism responsible for the coexistence between cooperators and defectors that is not present for $\phi = 0$. Interestingly, the presence of defectors is only possible if they form a percolating cluster and no finite cluster of defectors is stable: either they grow, merge with others, and span the whole lattice or the isolated cluster becomes extinct. This is our main result: finite-size cooperators and defectors, whose hard core is an effective, averaged interaction restraining their movements, are able to coexist over a broad region of the phase diagram only if defectors are organized in a interconnected cluster, a percolating sea of defectors. A similar effect was found for the public goods game played on a lattice with empty sites and no mobility [16]. It would be interesting to investigate whether this condition for coexistence between cooperators and defectors also occurs in lattice models, where excluded area is inherent to the formulation of the problem.

In this paper we have focused on the particular homogeneous case of equal sizes and equal velocities for both cooperators and defectors. Following Refs. [45] and [55], it is essential to explore the whole (S,T) parameter space and the dependence on the chosen dynamic rule in order to check the robustness of cooperation. Furthermore, several extensions are possible. For example, velocities may not be constant [29] and depend on the neighborhood [45] or strategy. The hard-core radius may also correlate with strategy, r_C and r_D for cooperators and defectors, respectively. In particular, if individuals coevolve with mutations, Is there an optimal equilibrium radii ratio to which the system converges or, instead, a permanent arms race? What are the effects of having size dispersion? If velocity and size coevolve along with strategies, defectors may become small and fast while cooperators become large and slow. Finally, what happens if there is a fraction of fundamentalists (both cooperators and defectors or just defectors) whose strategies or positions never change? In all these cases, it is important to study also the geometric properties of the interfaces between cooperator and defector clusters since these are the places where all strategy flips occur. From a more physical perspective, it would be interesting to find out, for each transition line, which dynamical universality class it belongs to [58]. These and other relevant questions are being considered.

ACKNOWLEDGMENTS

This research was partially supported by the Brazilian agencies CNPq, CAPES, and Fapergs. J.J.A. also thanks the INCT-Sistemas Complexos (CNPq) for partial support. We thank the supercomputing laboratory at Universidade Federal da Integração Latino-Americana (LCAD/Unila), where the simulations were run, for computer time.

[1] R. Axelrod, *The Evolution of Cooperation* (Basic Books, New York, 1984).
[2] M. A. Nowak and R. M. May, Nature **359**, 826 (1992).
[3] M. Doebeli and C. Hauert, Ecol. Lett. **8**, 748 (2005).
[4] M. A. Nowak, Science **314**, 1560 (2006).
[5] G. Szabó and G. Fáth, Phys. Rep. **446**, 97 (2007).
[6] C. P. Roca, J. A. Cuesta, and A. Sánchez, Phys. Life Rev. **6**, 208 (2009).
[7] M. Perc and A. Szolnoki, BioSystems **99**, 109 (2010).
[8] A. Traulsen, D. Semmann, R. D. Sommerfeld, H.-J. Krambeck, and M. Milinski, Proc. Natl. Acad. Sci. USA **107**, 2962 (2010).
[9] D. G. Rand, S. Arbesman, and N. A. Christakis, Proc. Natl. Acad. Sci. USA **108**, 19193 (2011).
[10] C. Gracia-Lázaro, A. Ferrer, G. Ruiz, A. Tarancon, J. A. Cuesta, A. Sánchez, and Y. Moreno, Proc. Natl. Acad. Sci. USA **109**, 12922 (2012).
[11] J. Grujic, T. Rohl, D. Semmann, M. Milinski, and A. Traulsen, PLOS One **7**, e47718 (2012).

[12] F. C. Santos and J. M. Pacheco, Phys. Rev. Lett. **95**, 098104 (2005).
[13] F. C. Santos, J. M. Pacheco, and T. Lenaerts, Proc. Natl. Acad. Sci. USA **103**, 3490 (2006).
[14] M. H. Vainstein and J. J. Arenzon, Phys. Rev. E **64**, 051905 (2001).
[15] M. Lin, N. Li, L. Tian, and D.-N. Shi, Physica A **389**, 1753 (2010).
[16] Z. Wang, A. Szolnoki, and M. Perc, Sci. Rep. **2**, 369 (2012).
[17] V. Colizza, A. Barrat, M. Barthélemy, and A. Vespignani, Proc. Natl. Acad. Sci. USA **103**, 2015 (2006).
[18] D. Helbing, I. Farkas, and T. Vicsek, Nature **407**, 487 (2000).
[19] S. Bouzat and M. N. Kuperman, Phys. Rev. E **89**, 032806 (2014).
[20] L. A. Dugatkin and D. S. Wilson, Am. Nat. **138**, 687 (1991).
[21] M. Enquist and O. Leimar, Anim. Behav. **45**, 747 (1993).
[22] R. Ferrière and R. E. Michod, Am. Nat. **147**, 692 (1996).
[23] S. J. Majeski, G. Linden, C. Linden, and A. Spitzer, Complexity **5**, 16 (1999).
[24] I. M. Hamilton and M. Taborsky, Proc. R. Soc. B **272**, 2259 (2005).
[25] J. C. Koella, Proc. R. Soc. B **267**, 1979 (2000).
[26] C. A. Aktipis, J. Theor. Biol. **231**, 249 (2004).
[27] J.-F. Le Galliard, F. Ferrière, and U. Dieckmann, Am. Nat. **165**, 206 (2005).
[28] L.-L. Jiang, W.-X. Wang, Y.-C. Lai, and B.-H. Wang, Phys. Rev. E **81**, 036108 (2010).
[29] H. Cheng, H. Li, Q. Dai, Y. Zhu, and J. Yang, New J. Phys. **12**, 123014 (2010).
[30] H.-X. Yang, Z.-X. Wu, and B.-H. Wang, Phys. Rev. E **81**, 065101(R) (2010).
[31] H. Cheng, Q. Dai, H. Li, Y. Zhu, M. Zhang, and J. Yang, New J. Phys. **13**, 043032 (2011).
[32] H. Lin, D.-P. Yang, and J. Shuai, Chaos Solitions Fractals **44**, 153 (2011).
[33] Y.-T. Lin, H.-X. Yang, Z.-X. Wu, and B.-H. Wang, Physica A **390**, 77 (2011).
[34] D. Helbing and W. Yu, Proc. Natl. Acad. Sci. USA **106**, 3680 (2009).
[35] W. Yu, Phys. Rev. E **83**, 026105 (2011).
[36] Y. Liu, X. Chen, L. Zhang, F. Tao, and L. Wang, Chaos Solitions Fractals **45**, 1301 (2012).
[37] P. Buesser, M. Tomassini, and A. Antonioni, Phys. Rev. E **88**, 042806 (2013).
[38] Z. Chen, J. Gao, Y. Cai, and X. Xu, Physica A **390**, 1615 (2011).
[39] J. Zhang, W.-Y. Wang, W.-B. Du, and X.-B. Cao, Physica A **390**, 2251 (2011).
[40] C. Zhang, J. Zhang, F. J. Weissing, M. Perc, G. Xie, and L. Wang, PloS One **7**, e35183 (2012).
[41] R. Cong, B. Wu, Y. Qiu, and L. Wang, PLOS One **7**, e35776 (2012).
[42] H. Cheng, Q. Dai, H. Li, X. Qian, M. Zhang, and J. Yang, Eur. Phys. J. B **86**, 127 (2013).
[43] G. Ichinose, M. Saito, H. Sayama, and D. S. Wilson, Sci. Rep. **3**, 1 (2013).
[44] C. Zhang, J. Zhang, and G. Xie, Chaos Solitions Fractals **59**, 103 (2014).
[45] A. Antonioni, M. Tomassini, and P. Buesser, J. Theor. Biol. **344**, 40 (2014).
[46] M. H. Vainstein, A. T. C. Silva, and J. J. Arenzon, J. Theor. Biol. **244**, 722 (2007).
[47] M. Droz, J. Szwabiński, and G. Szabó, Eur. Phys. J. B **71**, 579 (2009).
[48] E. A. Sicardi, H. Fort, M. H. Vainstein, and J. J. Arenzon, J. Theor. Biol. **256**, 240 (2009).
[49] S. Meloni, A. Buscarino, L. Fortuna, M. Frasca, J. Gómez-Gardeñes, V. Latora, and Y. Moreno, Phys. Rev. E **79**, 067101 (2009).
[50] S. Suzuki and H. Kimura, J. Theor. Biol. **287**, 42 (2011).
[51] P. E. Smaldino and J. C. Schank, Theor. Pop. Biol. **82**, 48 (2012).
[52] H. Yang and B. Wang, Chin. Sci. Bull. **56**, 3693 (2011).
[53] A. Gelimson, J. Cremer, and E. Frey, Phys. Rev. E **87**, 042711 (2013).
[54] Y. Wei, X. Wang, J. Liu, I. Nememan, A. H. Singh, H. Weiss, and B. R. Levin, Proc. Natl. Acad. Sci. USA **108**, 4047 (2011).
[55] M. H. Vainstein and J. J. Arenzon, Physica A **394**, 145 (2014).
[56] D. R. Amor and J. Fort, Phys. Rev. E **84**, 066115 (2011).
[57] Z. Wang, A. Szolnoki, and M. Perc, Phys. Rev. E **85**, 037101 (2012).
[58] H.-X. Yang, Z. Rong, and W.-X. Wang, New J. Phys. **16**, 013010 (2014).
[59] M. A. Nowak, S. Bonhoeffer, and R. M. May, Int. J. Bifurcat. Chaos **4**, 33 (1994).
[60] J. Quintanilla, S. Torquato, and R. M. Ziff, J. Phys. A: Math. Gen. **33**, L399 (2000).
[61] S. Mertens and C. Moore, Phys. Rev. E **86**, 061109 (2012).
[62] P. Balister, B. Bollobás, and M. Walters, Rand. Struct. Algor. **26**, 392 (2005).
[63] M. N. Kuperman and S. Risau-Gusman, Phys. Rev. E **86**, 016104 (2012).